NANO LETTERS

pubs.acs.org/NanoLett Letter

Wide-Field Super-Resolution Optical Fluctuation Imaging through Dynamic Near-Field Speckle Illumination

Young Choi,[▽] MinKwan Kim,[▽] ChungHyun Park, Jongchan Park, YongKeun Park,* and Yong-Hoon Cho*

Cite This: *Nano Lett.* 2022, 22, 2194–2201

Read Online

ACCESS | Metrics & More | Article Recommendations | Supporting Information

ABSTRACT: Stochastic optical fluctuation imaging (SOFI) generates super-resolution fluorescence images by emphasizing the positions of fluorescent emitters via statistical analysis of their on-and-off blinking dynamics. In SOFI with speckle illumination (S-SOFI), the diffraction-limited grain size of the far-field speckles prevents independent blinking of closely located emitters, becoming a hurdle to realize the full super-resolution granted by SOFI processing. Here, we present a surface-sensitive super-resolution technique exploiting dynamic near-field speckle illumination to bring forth the full super-resolving power of SOFI without blinking fluorophores. With our near-field S-SOFI technique, up to 2.8- and 2.3-fold enhancements in lateral spatial resolution are demonstrated with computational and experimental fluorescent test targets labeled with conventional fluorophores, respectively. Fluorescent beads separated by 175 nm are also super-resolved by near-field speckles of 150 nm grain size, promising sub-100 nm resolution with speckle patterns of much smaller grain size.

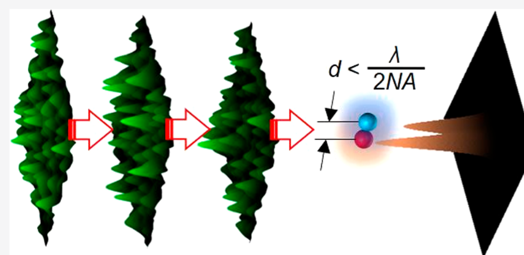

KEYWORDS: *super-resolution fluorescence microscopy, stochastic optical fluctuation imaging, dynamic speckle illumination, near-field speckle patterns*

INTRODUCTION

In optical microscopy, stochastic random processes have been regarded as detrimental noise sources and degrade the contrast and resolution of an optical image. For instance, when a coherent beam propagates through a path in the presence of dust particles or biological tissues with inhomogeneous refractive indexes, its wavefront randomly interferes upon facing many scatterers, resulting in a granular intensity pattern composed of the bright and dark dots, called speckles.[1] Speckle noise is notorious for corrupting the interferometric contrast of coherent imaging systems such as optical coherence tomography[1,2] and holographic microscopy.[1,3] In fluorescence microscopy, continuous observation of dynamic biological processes is often hindered by the random photoswitching of fluorophores.[4]

Both speckle phenomena[1−3] and fluorescence intermittency,[4] which always seem to be obstacles for the optical imaging, can be exploited for super-resolution imaging of fluorescent objects.[5] In joint use with advanced post-processing algorithms, a super-resolution image can be reconstructed by illuminating dynamic speckle patterns, which can act as random structured illuminations,[6] multiple measurement vectors for joint support recovery,[7] or external sources of fluorescence intensity fluctuation.[8] Meanwhile, the blinking of fluorescent point emitters has been extensively used to realize super-resolution imaging techniques, including single-molecule localization microscopy[9,10] and fluctuation analysis methods.[11−13] Hence, both speckles and fluorescence blinking provide examples of stochastic phenomena that can enhance imaging performance in combination with clever detection and analysis schemes.

Previously, a viable strategy of employing speckle-induced artificial fluorescence blinking to generate a super-resolution optical image has been suggested.[8] Stochastic optical fluctuation imaging (SOFI)[11] can yield a super-resolution image of fluorophore distributions by means of *dynamic speckle illumination*, such that local excitation intensity seen by individual fluorophores randomly fluctuates over time. SOFI analysis[11] and subsequent reweighting in the Fourier domain[14,15] turns the stack of speckle-fluctuated fluorescence images into a single super-resolution image. This speckle-based SOFI technique, termed as super-resolution optical fluctuation imaging with speckle patterns illumination (S-SOFI),[8] enhanced resolution of a fluorescence image by a factor of 1.6 beyond the diffraction limit. However, the moderate degree of resolution enhancement by S-SOFI technique is attributed

Received: October 8, 2021
Revised: February 18, 2022
Published: March 4, 2022

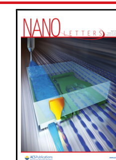

ACS Publications

© 2022 The Authors. Published by American Chemical Society

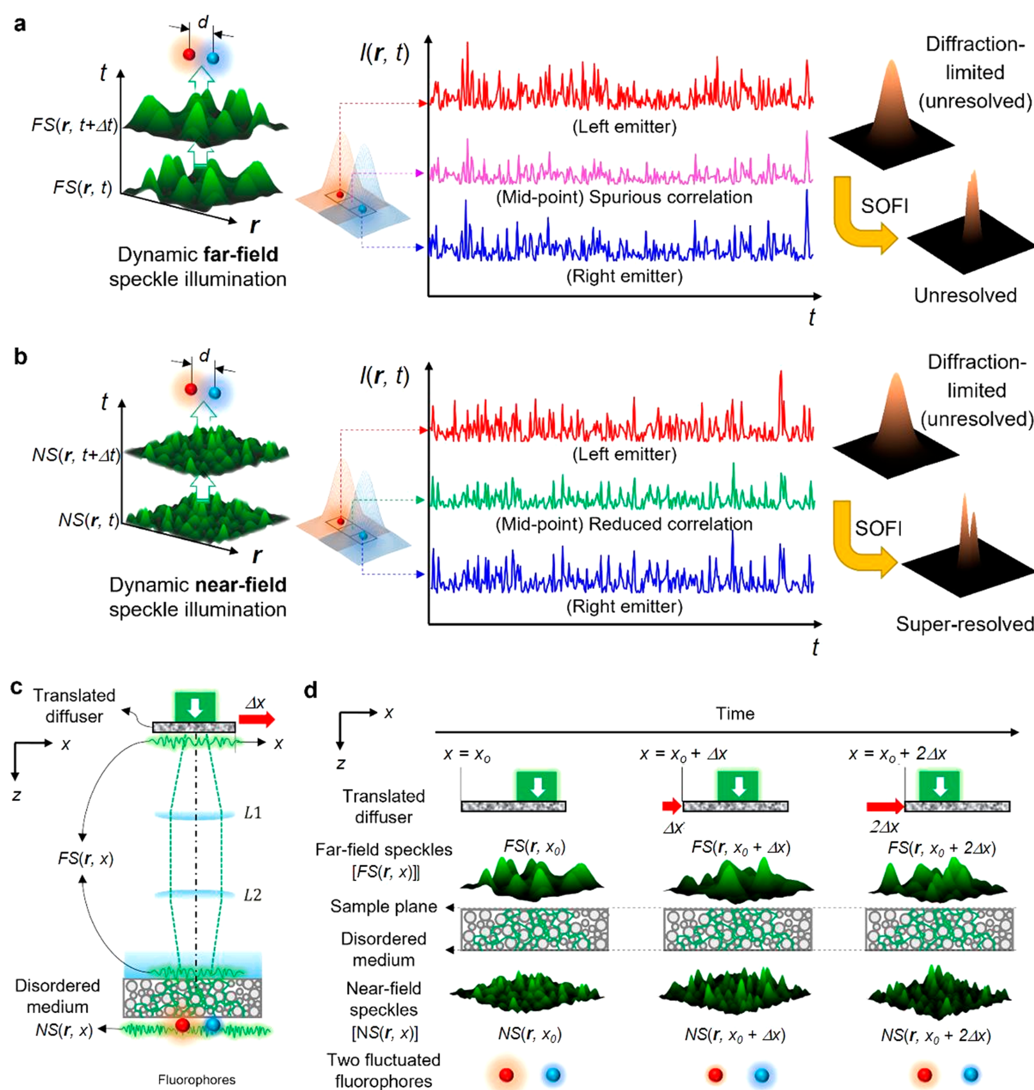

Figure 1. Dynamic near-field speckle illumination for NS-SOFI imaging experiment. (a, b) Two independent fluorophores are assumed to be separated within subdiffraction distance under dynamic speckle illumination in the far field (panel (a)) and near field (panel (b)). Examples of fluorescence intensity fluctuation trace $I(\mathbf{r},t)$ measured during 300 frames of dynamic speckle illumination sampled at the locations of the two fluorophores and their midpoint. In contrast to far-field speckles (panel (a)), dynamic near-field speckle illumination (panel (b)) of subwavelength grain size produces independent fluctuation of two fluorophores favorable for SOFI processing. Here, the transparent Gaussian lobes assigned to each fluorophore represent the scale of the point spread functions of the base fluorescence detection imaging system. (c) Schematic representation of illumination optics to produce dynamic near-field speckle illumination. A pair of (pseudocolored) red and blue sphere describes two independent fluorophores separated within subdiffraction distance under dynamic near-field speckle illumination. (d) Pictorial description of two-step scattering of a laser beam through the translated diffuser and turbid medium, which results in dynamic near-field speckle illumination at the sample plane (see Note S2 in the Supporting Information for details).

to the finite grain size[16] of the *far-field speckle* patterns, which are also diffraction-limited.

Introducing dynamic *near-field speckle* illumination[17−33] in S-SOFI endows new opportunities to realize a novel mode of wide-field subwavelength imaging. Subwavelength grain size of near-field speckle patterns increases the chances that fluorescent emitters separated even within subdiffraction distance experience different excitation intensity, well-approximating intrinsic blinking of the individual emitters, which is a crucial assumption to realize full resolution gain granted by SOFI processing.[11] Plus, by illuminating dynamic far-field speckle fields onto an easy-to-fabricate disordered medium without keeping spatial mode coupling constraints, dynamic near-field speckle patterns are readily produced.[34,35] This ease of implementation due to random nature of speckle fields is a clear advantage, compared to other super-resolution techniques utilizing regular-shaped near-field structured illumination such as near-field scanning optical microscopy (NSOM)[36−38] or localized plasmonic structured illumination microscopy (LPSIM).[39] Unlike previous approaches employing near-field speckle patterns and the transmission matrix,[35] SOFI enables facile reconstruction of super-resolution images without time-consuming calibration or a computationally heavy iterative image reconstruction process.

Here, we demonstrate the power of this new version of S-SOFI employing dynamic near-field speckle patterns; this is called the NS-SOFI technique. We begin with the motivation behind exploiting near-field speckle patterns to boost achievable resolution of traditional S-SOFI. The subwavelength extent of average grain size of the near-field speckle

https://doi.org/10.1021/acs.nanolett.1c03691
Nano Lett. 2022, 22, 2194−2201

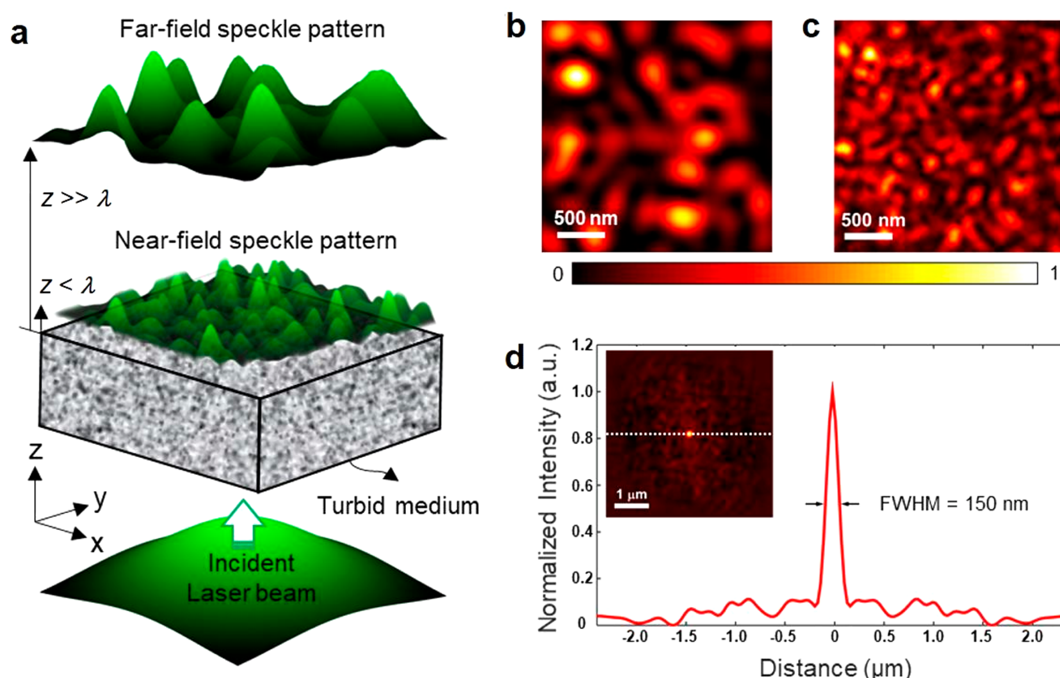

Figure 2. Comparison of speckle patterns in the far field and near field. (a) Diagrams comparing far-field and near-field speckle patterns. In contrast to far-field speckle patterns having propagated over a distance longer than a wavelength ($z \gg \lambda$), near-field speckle patterns occur within a sub-wavelength ($z < \lambda$) of the exit surface of a disordered medium, preserving evanescent high spatial-frequency Fourier components. (b,c) Measured intensity profiles of speckle patterns in the far field (panel (b)) and the near field (panel (c)). Color bars express normalized intensity. (d) Cross-sectional line profile along the dashed white line in the spatial autocorrelation image (inset) of the near-field speckle pattern (panel (c)).

patterns used in this study is characterized by a collection-mode NSOM.[17−22] Employing both simulative and experimental fluorescent resolution test targets, we evaluate the achievable super-resolution of the present method, suggesting its potential for application to super-resolution imaging of a thin fluorescent specimen.

■ RESULTS

In previous work,[8] the diffraction-limited grain size of the employed far-field speckle patterns was a major limitation to achieving the full resolution granted by the SOFI algorithm. This is because the cumulant operation defined in SOFI assumes vanishing mutual correlations between the fluorescence flickering of two individual emitters closely spaced within the subdiffraction distance.[11] As depicted in Figure 1a, however, if both emitters are illuminated by the same speckle grain, which is the case for far-field speckles of diffraction limited grain-size, their fluorescence intensities fluctuate in unison and are correlated. This undesired correlation violates the fundamental assumption of SOFI, which states that the two emitters must fluctuate independently. To eliminate this spurious correlation for acquiring full resolution benefit of the SOFI algorithm, the grain size of illuminating speckle patterns should be much smaller than the diffraction limit, as shown in Figure 1b, to realize mutually independent flickering of individual fluorophores. This subwavelength grain size is the unique feature of the near-field speckle patterns[17−33] and opens an opportunity to break the resolution limit of (far-field) S-SOFI[8] technique by approximating the speckle-fluctuated fluorescence to intrinsic blinking of the individual fluorescent labels.

As a simple means to generate the dynamic near-field speckle patterns exploited in our experiment, a disordered layer of white spray paint comprising TiO_2 nanoparticles and fixative polymer plays a dual role of a sample mount and wavefront shaper for near-field speckles as in Figure 1c. Figure 1d provides illustration of two-step scattering process for intuitive description of how a collimated laser beam turns into dynamic near-field speckle patterns through illumination optics system in Figure 1c. First, dynamic far-field speckle patterns [$\mathrm{FS}(\boldsymbol{r},x)$, $\boldsymbol{r}$ denotes the two-dimensional coordinates located at the sample plane and x assigns a position coordinate of the diffuser] are produced when a collimated laser beam is scattered by a translating diffuser. Next, these dynamic far-field speckle patterns enter the disordered medium after propagation through far-field lens system (depicted as L1, L2) and are scattered again within the disordered medium, thus turning into near-field speckle illumination [$\mathrm{NS}(\boldsymbol{r},x)$] at the sample plane. Dynamic variation of the near-field speckle patterns is due to independent far-field speckle patterns varying in sync with the movement of the diffuser ($x_0 \rightarrow x_0 + \Delta x \rightarrow x_0 + 2\Delta x$, as in Figure 1d).

In Figure 2, as a key enabler for realizing a new mode of S-SOFI, near-field speckle patterns are characterized in comparison with the diffraction-limited far-field speckle illumination employed in the previous work.[8] As shown in Figure 2a, the far-field speckle patterns propagate a distance of several wavelengths from the exit surface of disordered medium and can be easily measured using conventional optics. In contrast, near-field speckle patterns form within a sub-wavelength distance from the surface and consists of both propagating and evanescent modes. The latter mode is composed of subdiffraction spatial frequency components and results in the sub-wavelength spot size of the speckle grains when superposed with far-field speckle fields.[19] Figure 2c shows an example of near-field speckle pattern collected in an

https://doi.org/10.1021/acs.nanolett.1c03691
Nano Lett. 2022, 22, 2194−2201

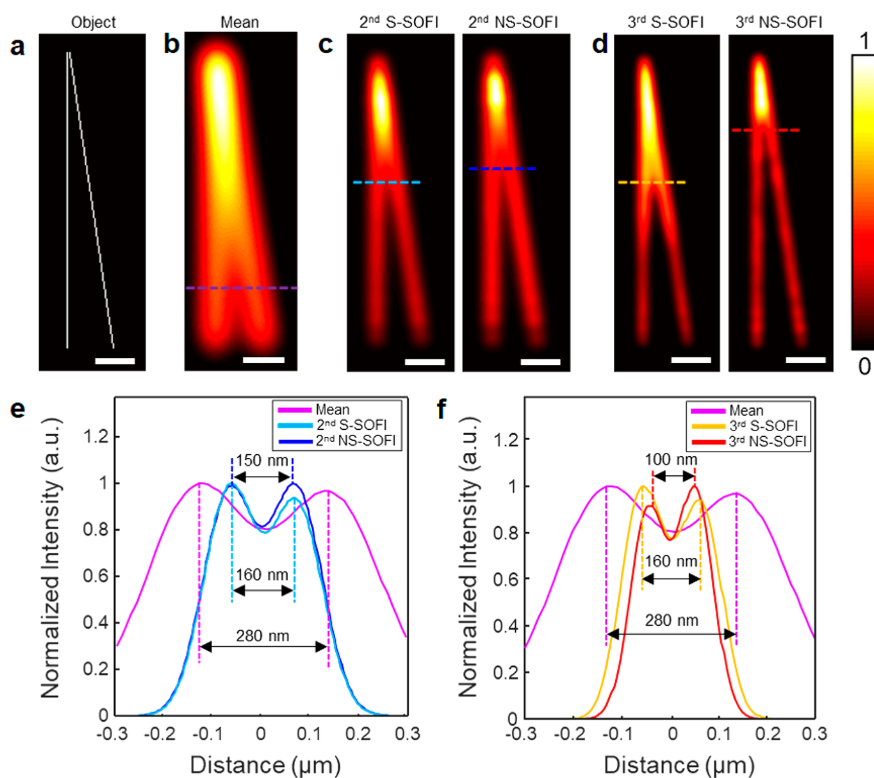

Figure 3. NS-SOFI resolution gain tested by computational test targets. (a) Two diverging filaments as the ground truth for our computational resolution test. (b) Mean image of the speckle-fluctuated image stack equivalent to a wide-field diffraction-limited image under uniform illumination. (c) The second-order S-SOFI images under far-field (left, 2nd S-SOFI) and near-field (right, 2nd NS-SOFI) speckle illumination. (d) Third-order S-SOFI images under far-field (left, 3rd S-SOFI) and near-field (right, 3rd NS-SOFI) speckle illumination. (e) Cross-sectional intensity profiles along linecuts over the mean image (panel (b)), 2nd S-SOFI image (panel (c), left), and 2nd NS-SOFI image (panel (c), right). (f) Cross-sectional intensity profiles along linecuts over the mean image (panel (b)), 3rd S-SOFI image (panel (d), left), and 3rd NS-SOFI image (panel (d), right). Scale bars in panels (a)−(d) = 300 nm.

arbitrary chosen 2.5 μm × 2.5 μm area over the surface of the disordered layer directly probed by a collection mode NSOM.[17−22] Contrary to the far-field speckle pattern in Figure 2b, spatial intensity variation in the near-field speckle pattern (Figure 2c) occurs over subdiffraction distance less than half of the excitation laser wavelength (λ_{laser} = 532 nm), which is impossible with diffraction-limited illumination.

Figure 2d presents the two-dimensional spatial autocorrelation image of the near-field speckle pattern in Figure 2c. The full-width at half-maximum (FWHM) of the autocorrelation in the inset graph of Figure 2d, or equivalently short-range correlation length of spatial intensity distribution, provides an estimate of the minimum grain size of the near-field speckle patterns.[40] The cross-sectional profile shows that our near-field speckle patterns have a correlation length of 150 nm significantly smaller than the half wavelength of the excitation laser. The actual correlation length can be even smaller than the measured value (150 nm), since no correction is applied to take into account of additional blur caused by the finite aperture size of the NSOM tip (see Section S1 in the Supporting Information). This sub-wavelength-scale grain size is the unique feature of near-field speckle patterns whose correlation length is driven by the microstructure of the scattering medium, not by the wavelength of the scattered light.[19−33] Unlike far-field speckle illumination with complex field exhibiting Rayleigh statistics, although dynamic near-field speckle illumination employed for NS-SOFI deviates from Rayleigh statistics (see Figure S2.2 in the Supporting Information),[19−33] the intensity statistics of speckle illumination that directly translates to the final super-resolution is the grain size, not the type of the speckle field statistics.

A simple computational experiment justifies the hypothesis aforementioned in Figure 1, as illustrated in Figure 3. Two filaments of increasing separation (Figure 3a, as the ground truth), on which a continuum of fluorophores of unit brightness are assumed to be labeled, provide an intuitive measure of the lateral spatial resolution. The brightness of this computational test target is modulated by a set of calculated speckle patterns (see detailed simulation workflow in Section S3 in the Supporting Information). To evaluate how the speckle grain size affects the achievable resolution of S-SOFI technique, we perform NS-SOFI imaging simulation with two sets of the speckle patterns convolved with illumination PSF having different FWHM values of 280 and 150 nm, corresponding to the far-field (identical to the diffraction limit of this simulation) and near-field speckle patterns (identical to the value measured in Figure 2d), respectively. Lateral spatial resolution of the resulting fluorescence images is calibrated as the minimum separation at which the dip visibility of a doubly peaked cross-sectional intensity profile reaches 0.1, corresponding to an ∼20% dip with respect to the peak intensity (for the exact definition, see Section S4 in the Supporting Information and ref 41). Resolution gain is defined as the ratio of the distances that achieves dip-visibility of 0.1 before and after NS-SOFI processing. The cautions regarding

https://doi.org/10.1021/acs.nanolett.1c03691
Nano Lett. 2022, 22, 2194−2201

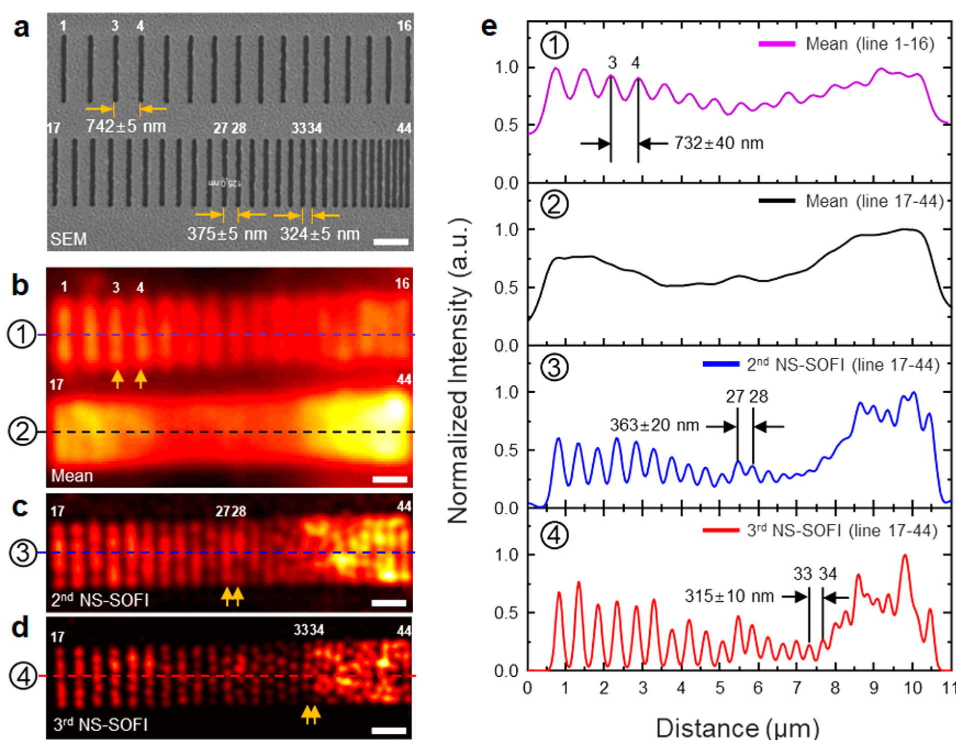

Figure 4. Experimental test of resolution enhancement with NS-SOFI technique. (a) SEM image of a ruler pattern milled on a 30-nm-thick gold layer deposited on top of a coverslip. Each line dip is labeled with fluorescent colloidal quantum dots to provide a reference length for fluorescence imaging system under test. Total of 44 lines are numbered as indicators of the individual lines. (b) A diffraction-limited mean image is defined as the average of a set of fluorescent images acquired under dynamic near-field speckle patterns. (c, d) 2nd and 3rd NS-SOFI images of the fluorescent line arrays in the second row (from lines 17−44). (e) Cross-sectional intensity profiles taken over the mean (panel (b)) and 2nd and 3rd NS-SOFI images (panels (c) and (d)). More than 20 intensity profiles are taken in parallel to the dashed lines ("①", purple; "②", black; "③", blue; and "④", red) and then averaged to produce a single representative intensity profile, as shown in panel (e), from which the lateral spatial resolution of each fluorescent image is measured. Scale bars in panels (a)−(d) = 1 μm.

line-cut-based resolution calibration are noted in Supporting Note S5 in the Supporting Information.

Figure 3c shows the second-order S-SOFI images generated by applying second-order SOFI processing to the fluorescence image stack fluctuated by both far-field (left, "2nd S-SOFI") and near-field (right, "2nd NS-SOFI") speckle patterns. As seen in the cross-sectional intensity profiles taken in Figure 3c, the 2nd NS-SOFI image achieves a resolution gain of 1.87-fold (= 280 nm ÷ 150 nm) enhancement, slightly higher than that of 1.75-fold (= 280 nm ÷ 160 nm) enhancement for the 2nd S-SOFI image (see Figure 3e).

The benefits of employing near-field speckle patterns for S-SOFI is much clearly demonstrated by additional resolution gain acquired when we apply third-order SOFI processing, as shown in Figure 3d. The dip visibility of the linecuts on the two third-order SOFI images, "3rd S-SOFI" and "3rd NS-SOFI" in Figure 3d, is evaluated in Figure 3f to compare their resolution gains. For the 3rd NS-SOFI image, near-field speckle patterns enable much higher resolution enhancement by a factor of 2.8 (= 280 nm ÷ 100 nm), while the resolution gain of the 3rd S-SOFI image remains at 1.75 (= 280 nm ÷ 160 nm), the same as that of the 2nd S-SOFI image. The 2.8-fold resolution gain achieved in the 3rd NS-SOFI images is close to the theoretical super-resolution of third-order SOFI algorithm applied to independently blinking emitters, namely, a 3-fold enhancement in resolution. Thus, the sub-wavelength grain size of the employed dynamic speckle illumination approximates fluorescence fluctuation to that of intrinsic blinking of adjacent emitters; it also successfully eliminates the spurious correlation that was problematic when the diffraction-limited far-field speckle patterns are employed for illumination.

The trend analyzed by the computational experiment in Figure 3 is also consistent with NS-SOFI imaging experiment performed in real-world setting with fluorescent ruler patterns, whose results are summarized in Figure 4. Diffraction-limited resolution is readily identified by inspecting lines 3 and 4 in the first row of the ruler pattern (Figure 4a, lines 1−16). The dip visibility of 0.1 is achieved at the separation of 732 ± 40 nm, whose actual distance is 742 ± 5 nm in the SEM image of Figure 4a and sets the actual diffraction limit of the fluorescent imaging system. The ruler patterns in the second row (lines 17−44) are not resolved in the mean image (Figure 4b and the second row of Figure 4e) due to the lack of resolution in our diffraction-limited imaging system.

NS-SOFI technique successfully resolves the line arrays in the second row of ruler patterns as shown in Figures 4c and 4d. As confirmed in the 2nd NS-SOFI image (Figure 4c) and the blue intensity profile at the third row (Figure 4e), the dip visibility of 0.1 is achieved between lines 27 and 28, corresponding to 363 ± 20 nm separation (compared to the actual distance of 375 ± 5 nm in SEM image). Compared to the diffraction limit of 742 ± 5 nm, the 2nd NS-SOFI image resolution is enhanced 1.98-fold (= 742 nm ÷ 375 nm). Hence, the 2nd NS-SOFI image achieves ideal 2-fold resolution gain, which is possible only with blinking fluorescent labels. This result confirms that near-field speckle patterns indeed approximate the intrinsic blinking of the fluorophores, because of its sub-wavelength grain size.

https://doi.org/10.1021/acs.nanolett.1c03691
Nano Lett. 2022, 22, 2194−2201

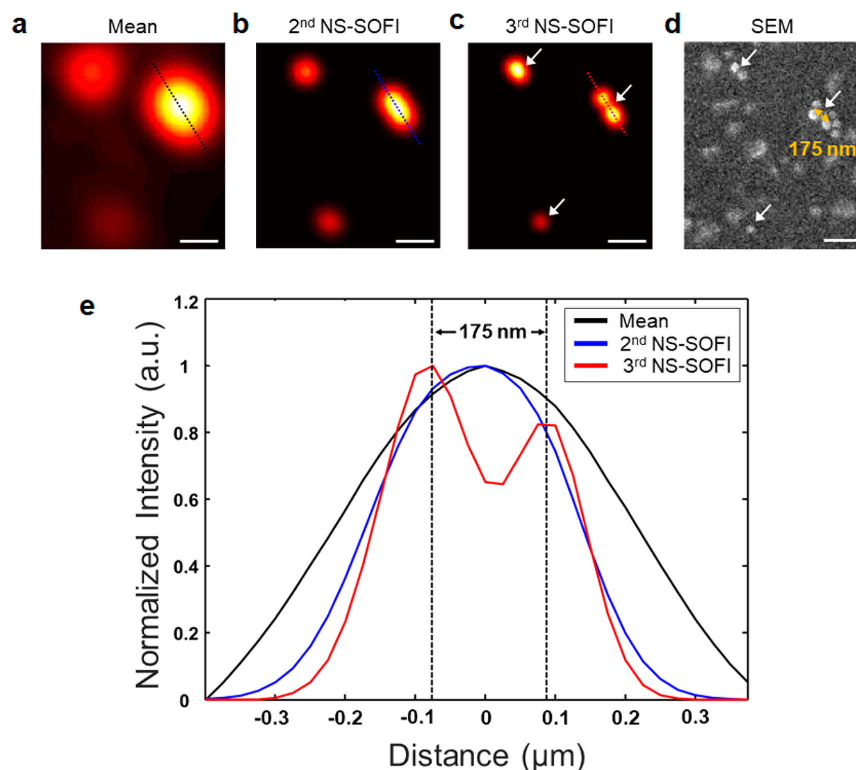

Figure 5. Resolution enhancement with NS-SOFI technique using fluorescent beads with emission wavelengths of 560 nm. (a) Mean (diffraction-limited resolution), (b) 2nd NS-SOFI and (c) 3rd NS-SOFI super-resolution images of the same region of interest. Intensity profiles are taken along the dashed lines in each image to compare the resolution. (d) SEM image reveals the true location of fluorescent beads in the same field-of-view of optical images (panels (a)−(c)). The white arrows indicate the corresponding positions of the beads in the 3rd NS-SOFI image. (e) Three intensity profiles taken along the dashed lines in optical images (panels (a)−(c)). Fluorescent beads separated by 175 nm are resolved by third-order NS-SOFI processing (solid red lines in (panel (e)). Scale bars for panels (a)−(d) = 500 nm.

As demonstrated by simulation (Figure 3), the resolution benefit of near-field speckle patterns is more prominent with the use of third-order SOFI processing. For example, the 3rd NS-SOFI image in Figure 4d resolves lines 33 and 34, separated 315 ± 10 nm (324 ± 5 nm in the SEM image) with a dip visibility of 0.1, experimentally achieving 2.3-fold (= 742 nm ÷ 324 nm) resolution enhancement over the diffraction-limited mean image. Although this improvement (measured for ruler patterns of discretely varying separation) is lower than the 2.8-fold gain expected in the simulated 3rd NS-SOFI image of Figure 3d (for the two filaments of continuously increasing separation), a better than 2-fold resolution enhancement without using blinking fluorescent labels is feasible only when near-field speckle patterns modulate the brightness of fluorophores.

Unlike the fluorescent ruler patterns in Figure 4 representing a predefined structure useful for accurate calibration of image resolution, the practicality of NS-SOFI is demonstrated by its performance tested on the fluorescent sample with unknown structures such as randomly dry-casted fluorescent beads. Figure 5 shows the results of an NS-SOFI imaging experiment with fluorescent beads 100 nm in diameter, successfully resolving a pair of beads separated by 175 nm, the subdiffraction distance of which is clearly less than half of the emission wavelength of the fluorescent beads (λ_{bead} = 560 nm) and thus, not resolved in the diffraction-limited imaging system. This is close to the minimum resolution possible with near-field speckle patterns with 150 nm grain size (Figure 2d) employed in the current system[34,35] as the absolute resolution of NS-SOFI technique is ultimately limited by the speckle grain size, which can be considered to be the minimum distance at which two fluorescence emitters can experience mutually random excitation intensity. It has recently been shown that near-field speckle patterns with a grain size of <100 nm can be generated in other subwavelength platforms such as a multilayer hyperbolic metamaterial.[42] Hence, the super-resolution record of 175 nm in Figures 5c and 5e does not set an ultimate limit of the NS-SOFI technique. Realizing sub-100 nm resolution via NS-SOFI technique is within technical reach and reduces to an engineering issue of designing a subwavelength interface that generates near-field speckle patterns with as small a grain size as possible.

DISCUSSION

One of the advantages of using near-field speckle patterns is the easy excitation of wide-field near-field illumination without stringent spatial mode coupling constraints. As the generation of speckle patterns is based on multiple scattering of coherent wavefronts through the disordered dielectric nanomaterials, no strict spatial or momentum matching conditions need to be met for the incident beams. This contrasts with the structured illumination microscopy (SIM) techniques relying on the regular-shaped structured near-field illumination such as LPSIM,[39] where the excitation of subwavelength-scale structured illumination results from constructive interference under tight modal coupling constraints posed on both illumination geometry and wavelengths. In contrast, the only requirement for mode matching with disordered media is posed on the temporal coherence of the illumination beam.

This is because other spectral components with frequency detuning larger than the temporal correlation length[43] of the disordered medium generate independent speckle patterns and thus blur the contrast of the original speckle pattern upon superposition of multiple uncorrelated speckle patterns.

Employing wide-field random illumination for super-resolution considerably relaxes the difficulty of implementing illumination hardwares, which is particularly challenging under near-field illumination conditions. Using speckle illumination in combination with fluctuation imaging not only lowers the cost of hardware implementation, but also aids microscopy practictioners to avoid the potential artifacts originating from mechanical instability of illuminating hardware or distortion of illumination profiles during reconstruction of a super-resolution image. For instance, in NSOM,[36−38] closed-loop nanoscale positioning hardware strictly control the low-throughput tip probe to keep its axial distance from the sample surface. This is because NSOM image resolution can deteriorate by axial diffraction of subwavelength focal spot, which must be avoided during long scanning time.[36] SIM reconstructions are particularly prone to image artifacts produced by distortion of illumination profiles, which can occur due to imperfections of the illuminating devices.[44−46] For this reason, it is difficult to avoid SIM artifacts in LPSIM[39] because wide-field localized plasmonic illumination produced by plasmonic antenna arrays are susceptible to lithographic fabrication errors. In addition, efficient coupling of an incoming beam into plasmonic arrays requires active control of polarization, wavefront or beam steering, further increasing the complexity of the illumination optics.[39,47−50] In NS-SOFI, however, the sample is mounted on top of the disordered medium, where near-field speckle patterns are readily produced by the scattering of far-field speckle patterns incident on the backside of the same disordered medium. Hence, if the fluorescent sample is not thicker than decay length of the evanescent near-field speckle patterns, we can safely assume that the sample is always excited under near-field speckle illumination. Plus, fluctuation-based super-resolution methods such as SOFI requires only the statistics of the speckle illumination, not any particular illumination profiles for artifact-free image construction.

Like any super-resolution methods employing near-field illumination, the sample volume where NS-SOFI-based super-resolution is effective is restricted to the surface of the disordered media. This limit comes from the fact that near-field speckle patterns quickly blur upon propagation from the exit surface of the disordered media and become far-field speckle patterns of diffraction-limited grain size. Therefore, one of the ideal samples for NS-SOFI would be fluorescent emitters hosted within a specimen having a thickness less than half of the illumination wavelength. For instance, quantum emitters within atomically thin solid-state materials such as hexagonal boron nitrides[51] and transition-metal dichalcogenide monolayers meet our imaging requirements. We envision that this practical application will perfectly apply the super-resolving power of the NS-SOFI technique.

ASSOCIATED CONTENT

Supporting Information

All the data supporting our findings are presented in the main text and the Supporting Information. The MATLAB codes are available from corresponding author upon reasonable request.

The Supporting Information is available free of charge at https://pubs.acs.org/doi/10.1021/acs.nanolett.1c03691.

Supporting figures and notes S1−S6 (PDF)

AUTHOR INFORMATION

Corresponding Authors

YongKeun Park − *Department of Physics, Korea Advanced Institute of Science and Technology (KAIST), Daejeon 34141, Republic of Korea; KAIST, Institute for Health Science and Technology, Daejeon 34141, Republic of Korea; Tomocube, Inc., Daejeon 34051, Republic of Korea;* orcid.org/0000-0003-0528-6661; Phone: (82) 42-350-2514; Email: yk.park@kaist.ac.kr

Yong-Hoon Cho − *Department of Physics, Korea Advanced Institute of Science and Technology (KAIST), Daejeon 34141, Republic of Korea; KAIST Institute for the NanoCentury, KAIST, Daejeon 34141, Republic of Korea;* orcid.org/0000-0002-7701-8562; Phone: (82) 42-350-2549; Email: yhc@kaist.ac.kr

Authors

Young Choi − *Department of Physics, Korea Advanced Institute of Science and Technology (KAIST), Daejeon 34141, Republic of Korea*

MinKwan Kim − *Department of Physics, Korea Advanced Institute of Science and Technology (KAIST), Daejeon 34141, Republic of Korea; Graduate School of Nanoscience and Technology, KAIST, Daejeon 34141, Republic of Korea*

ChungHyun Park − *Department of Physics, Korea Advanced Institute of Science and Technology (KAIST), Daejeon 34141, Republic of Korea; KAIST Institute for the NanoCentury, KAIST, Daejeon 34141, Republic of Korea*

Jongchan Park − *Department of Physics, Korea Advanced Institute of Science and Technology (KAIST), Daejeon 34141, Republic of Korea;* Present Address: Department of Bioengineering, University of California, Los Angeles, CA 90095, USA (J.-C. Park); orcid.org/0000-0002-0999-6778

Complete contact information is available at: https://pubs.acs.org/10.1021/acs.nanolett.1c03691

Author Contributions

[∇]These authors contributed equally to this work.

Notes

The authors declare no competing financial interest.

ACKNOWLEDGMENTS

This work was supported by the National Research Foundation of the Korean government (Nos. 2019R1A2B5B03070642, 2020M3E4A1080112, 2017R1A6A3A11036019, 2015R1A3A2066550), KAIST End-Run Program funded by the Ministry of Science and ICT in 2017 (No. N11170044), and Samsung Science and Technology Foundation (under Project No. SSTF-BA1602-05).

REFERENCES

(1) Goodman, J. W. *Speckle Phenomena in Optics: Theory and Applications*; Roberts and Company Publishers, 2007.

(2) Schmitt, J. M.; Xiang, S. H.; Yung, K. M. Speckle in optical coherence tomography. *J. Biomed. Opt.* **1999**, *4* (1), 95−105.

(3) Bianco, V.; Memmolo, P.; Leo, M.; Montresor, S.; Distante, C.; Paturzo, M.; Picart, P.; Javidi, B.; Ferraro, P.; et al. Strategies for

reducing speckle noise in digital holography. *Light: Sci. Appl.* **2018**, *7* (1), 1−16.
(4) Ha, T.; Tinnefeld, P. Photophysics of Fluorescent Probes for Single-Molecule Biophysics and Super-Resolution Imaging. *Annu. Rev. Phys. Chem.* **2012**, *63*, 595−617.
(5) Schermelleh, L.; et al. Super-resolution microscopy demystified. *Nat. Cell Biol.* **2019**, *21*, 72−84.
(6) Mudry, E.; et al. Structured illumination microscopy using unknown speckle patterns. *Nat. Photonics* **2012**, *6*, 312−315.
(7) Min, J.; Jang, J.; Keum, D.; Ryu, S.-W.; Choi, C.; Jeong, K.-H.; Ye, J. C. Fluorescent microscopy beyond diffraction limits using speckle illumination and joint support recovery. *Sci. Rep.* **2013**, *3*, 1−6.
(8) Kim, M.; Park, C.; Rodriguez, C.; Park, Y.; Cho, Y.-H. Superresolution imaging with optical fluctuation using speckle patterns illumination. *Sci. Rep.* **2015**, *5*, 16525.
(9) Betzig, E.; et al. Imaging intracellular fluorescent proteins at nanometer resolution. *Science* **2006**, *313*, 1642−1645.
(10) Rust, M. J.; Bates, M.; Zhuang, X. Sub-diffraction-limit imaging by stochastic optical reconstruction microscopy (STORM). *Nat. Methods* **2006**, *3*, 793−795.
(11) Dertinger, T.; Colyer, R.; Iyer, G.; Weiss, S.; Enderlein, J. Fast, background-free, 3D super-resolution optical fluctuation imaging (SOFI). *Proc. Natl. Acad. Sci. U. S. A.* **2009**, *106*, 22287−22292.
(12) Gustafsson, N.; Culley, S.; Ashdown, G.; Owen, D. M.; Pereira, P. M.; Henriques, R.; et al. Fast live-cell conventional fluorophore nanoscopy with ImageJ through super-resolution radial fluctuations. *Nat. Commun.* **2016**, *7*, 1−9.
(13) Yahiatene, I.; Hennig, S.; Müller, M.; Huser, T. Entropy-based super-resolution imaging (ESI): from disorder to fine detail. *ACS Photon* **2015**, *2*, 1049−1056.
(14) Geissbuehler, S.; Bocchio, N. L; Dellagiacoma, C.; Berclaz, C.; Leutenegger, M.; Lasser, T. Mapping molecular statistics with balanced super-resolution optical fluctuation imaging (bSOFI). *Opt. Nanoscopy* **2012**, *1*, 4.
(15) Dertinger, T.; Colyer, R.; Vogel, R.; Enderlein, J.; Weiss, S. Achieving increased resolution and more pixels with Superresolution Optical Fluctuation Imaging (SOFI). *Opt. Express* **2010**, *18*, 18875.
(16) Here, the grain size of a speckle is defined as the full width at half-maximum of the autocorrelation function of speckle intensity. For details, see Chapter 4 in ref 1.
(17) Apostol, A.; Dogariu, A. Spatial correlations in the near field of random media. *Phys. Rev. Lett.* **2003**, *91*, 093901.
(18) Emiliani, V.; Intonti, F.; Cazayous, M.; Wiersma, D. S.; Colocci, M.; Aliev, F.; Lagendijk, A. Near-field short range correlation in optical waves transmitted through random media. *Phys. Rev. Lett.* **2003**, *90*, 250801.
(19) Parigi, V.; Perros, E.; Binard, G.; Bourdillon, C.; Maitre, A.; Carminati, R.; Krachmalnicoff, V.; De Wilde, Y.; et al. Near-field to far-field characterization of speckle patterns generated by disordered nanomaterials. *Opt. Express* **2016**, *24* (7), 7019−7027.
(20) Naraghi, R. R.; Sukhov, S.; Dogariu, A. Disorder fingerprint: intensity distributions in the near field of random media. *Phys. Rev. B* **2016**, *94* (17), 174205.
(21) Naraghi, R. R.; Cançado, L. G.; Salazar-Bloise, F.; Dogariu, A. Near-field coherence reveals defect densities in atomic monolayers. *Optica* **2017**, *4* (5), 527.
(22) Cançado, L. G.; Naraghi, R. R.; Dogariu, A. Passive near-field imaging with pseudo-thermal sources. *Opt. Lett.* **2017**, *42* (6), 1137.
(23) Carminati, R. Subwavelength spatial correlations in near-field speckle patterns. *Phys. Rev. A - At. Mol. Opt. Phys.* **2010**, *81*, 1−5.
(24) Dogariu, A.; Carminati, R. Electromagnetic field correlations in three-dimensional speckles. *Phys. Rep.* **2015**, *559*, 1−29.
(25) Apostol, A.; Dogariu, A. Coherence properties near interfaces of random media. *Phys. Rev. E* **2003**, *67* (5), 055601.
(26) Apostol, A.; Dogariu, A. First-and second-order statistics of optical near fields. *Opt. Lett.* **2004**, *29* (3), 235−237.
(27) Apostol, A.; Dogariu, A. Non-Gaussian statistics of optical near-fields. *Phys. Rev. E - Stat., Nonlinear, Soft Matter Phys.* **2005**, *72* (2), 025602.
(28) Chen, X.; Zhang, Y.; Han, Y.; Rong, Z.; Zhang, L.; Li, Z.; Cheng, C. Study on the correspondence between random surface topography and its interface speckle field. *Opt. Commun.* **2020**, *462*, 125308.
(29) Henkel, C.; Joulain, K.; Carminati, R.; Greffet, J. J. Spatial coherence of thermal near fields. *Opt. Commun.* **2000**, *186* (1−3), 57−67.
(30) Roychowdhury, H.; Wolf, E. Effects of spatial coherence on near-field spectra. *Opt. Lett.* **2003**, *28* (3), 170−172.
(31) Bender, N.; Yılmaz, H.; Bromberg, Y.; Cao, H. Creating and controlling complex light. *APL Photonics* **2019**, *4* (11), 110806.
(32) Bender, N.; Yılmaz, H.; Bromberg, Y.; Cao, H. Customizing speckle intensity statistics. *Optica* **2018**, *5* (5), 595−600.
(33) Bromberg, Y.; Cao, H. Generating non-Rayleigh speckles with tailored intensity statistics. *Phys. Rev. Lett.* **2014**, *112* (21), 213904.
(34) Park, J. H.; et al. Subwavelength light focusing using random nanoparticles. *Nat. Photonics* **2013**, *7*, 454−458.
(35) Park, C. H.; et al. Full-field subwavelength imaging using a scattering superlens. *Phys. Rev. Lett.* **2014**, *113*, 113901.
(36) Betzig, E.; Trautman, J. K. Near-field optics: microscopy, surface modification beyond the limit diffraction. *Science* **1992**, *257*, 189−195.
(37) Strinkovski, A.; et al. Near-field optics: from subwavelength illumination to nanometric shadowing. *Nat. Biotechnol.* **2003**, *21*, 1378−1386.
(38) Lukas Novotny, B. H. *Principle of Nano-optics*; Cambridge University Press, 2012.
(39) Ponsetto, J. L.; et al. Experimental demonstration of localized plasmonic structured illumination microscopy. *ACS Nano* **2017**, *11*, 5344−5350.
(40) Shapiro, B. Large intensity fluctuations for wave propagation in random media. *Phys. Rev. Lett.* **1986**, *57*, 2168−2171.
(41) Geissbuehler, S.; Dellagiacoma, C.; Lasser, T. Comparison between SOFI and STORM. *Biomed. Opt. Express* **2011**, *2*, 408.
(42) Lee, Y. U.; Zhao, J.; Ma, Q.; Khorashad, L. K.; Posner, C.; Li, G.; Wisna, G. B. M.; Burns, Z.; Zhang, J.; Liu, Z.; et al. Metamaterial assisted illumination nanoscopy via random super-resolution speckles. *Nat. Commun.* **2021**, *12*, 1559.
(43) Mosk, A. P.; Lagendijk, A.; Lerosey, G.; Fink, M. Controlling waves in space and time for imaging and focusing in complex media. *Nat. Photonics* **2012**, *6*, 283−292.
(44) Ströhl, F.; Kaminski, C. F. Frontiers in structured illumination microscopy. *Optica* **2016**, *3*, 667.
(45) Ball, G.; Demmerle, J.; Kaufmann, R.; Davis, I.; Dobbie, I. M.; Schermelleh, L.; et al. SIMcheck: A toolbox for successful super-resolution structured illumination microscopy. *Sci. Rep.* **2015**, *5*, 1−12.
(46) Müller, M.; et al. Strategic and practical guidelines for successful structured illumination microscopy. *Nat. Protoc.* **2017**, *12*, 988−1010.
(47) Ertsgaard, C. T.; McKoskey, R. M.; Rich, I. S.; Lindquist, N. C. Dynamic placement of plasmonic hotspots for super-resolution surface-enhanced Raman scattering. *ACS Nano* **2014**, *8*, 10941−10946.
(48) Gjonaj, B.; et al. Active spatial control of plasmonic fields. *Nat. Photonics* **2011**, *5*, 360−363.
(49) Bayer, D.; et al. Adaptive subwavelength control of nano-optical fields. *Nature* **2007**, *446*, 301−304.
(50) Zhang, X.; et al. Broadband two-dimensional manipulation of surface plasmons. *Nano Lett.* **2009**, *9*, 462−466.
(51) Feng, J.; et al. Imaging of optically active defects with nanometer resolution. *Nano Lett.* **2018**, *18*, 1739−1744.

https://doi.org/10.1021/acs.nanolett.1c03691
Nano Lett. 2022, 22, 2194−2201